

1 **Improved microextraction of selected triazines using polymer monoliths modified**
2 **with carboxylated multi-walled carbon nanotubes**

3 *Beatriz Fresco-Cala, Soledad Cárdenas, Miguel Valcárcel**

4 *Department of Analytical Chemistry, Institute of Fine Chemistry and Nanotechnology,*
5 *Marie Curie Building, Campus of Rabanales, University of Córdoba, 14071, Córdoba,*
6 *Spain.*

7 **Abstract**

8 This article reports on the enhancement of the capacity of an acrylate-based monolithic
9 solid sorbent by anchoring carboxylated multi-walled carbon nanotubes (c-MWCNTs) in its
10 pores and on its surface. Monolithic poly(butyl acrylate-*co*-ethyleneglycol dimethacrylate)
11 [poly(BA-*co*-EGDMA)] was synthesized inside a fused silica capillary via free-radical
12 polymerization, and an ethanolic dispersion of c-MWCNTs was passed through the
13 capillary. The resulting poly(BA-*co*-EGDMA-c-MWCNTs) monolith was characterized by
14 scanning electron microscopy to confirm the presence of the c-MWCNTs. The effect of
15 using three different kinds of carbon nanoparticles and the microextraction step were
16 studied using triazine herbicides as model compounds. The use of c-MWCNTs resulted in
17 best performance in terms of extraction enhancement (compared to carboxylated single-
18 walled carbon nanotubes and oxidized single-walled carbon nanohorns). The use of these
19 carbon nanoparticles improved the extraction of triazines in any case when compared to
20 using a bare poly(BA-*co*-EGDMA) monolith. The triazines were then quantified by gas
21 chromatography with mass spectrometric detection. Detection limits ranged from 0.03 to
22 0.1 $\mu\text{g}\cdot\text{L}^{-1}$ (except for simazine; 0.6 $\mu\text{g}\cdot\text{L}^{-1}$), and the precision (relative standard deviation)

23 varied between 3.0 and 11.4%. The reproducibility between units is <14.3% (expressed as
24 relative standard deviation) which demonstrates the robustness of the method. The method
25 was applied to analyze an unknown sample of orange juice and gave a value of 0.18 $\mu\text{g}\cdot\text{L}^{-1}$
26 for prometryn. Finally, the analysis of spiked samples of water and orange juices yielded
27 recoveries ranging from 81 to 113% and 75 to 125%, respectively.

28 **Keywords:** *Monolithic solid, carboxylated multi-walled carbon nanotubes, (micro)solid*
29 *phase extraction, triazines, water, orange juice.*

30 *Corresponding author. Phone and fax: +34 957218616 email: galvacam@uco.es

31

32

33

34

35

36

37

38

39

40

41

42 **Running title:** Poly(BA-co-EGDMA-c-MWCNTs) monolith as a microextraction unit

43

44 **Introduction**

45 Sample preparation has been the focus of intense research in order to improve the isolation
46 and preconcentration steps of the analytical procedures. Current trends in this context
47 involve the simplification and miniaturization of separation techniques in both solid and
48 liquid phase formats. The success of these tendencies depends on the efficiency of the
49 extracting medium [1]. Nanostructured materials can be identified as a turning point on the
50 development of new miniaturized approaches [2], as they are more efficient than silica-
51 based or polymeric sorbents due to their high aspect ratio and chemical nature.

52 Monoliths are a continuous piece of a highly porous material, allowing solvents to flow
53 through their large pores (>50 nm macropores, 2-50 nm mesopores). The monoliths can be
54 classified in three types: polymer monoliths [3], silica-based monoliths [4] and organic-
55 silica hybrid monoliths [5]. In the chromatographic and electrophoretic context, these
56 materials have some advantages over particle packed columns such as: easy synthesis,
57 mechanical stability and direct linkage of the solid with the inner walls of the support.
58 Besides, they feature tolerance to high flows allowing fast separations of target analytes,
59 much more efficient mass transfer, great diversity in shapes and supports and good
60 synthesis reproducibility. Due to their versatility, sorbent monoliths have been used to
61 improve chromatographic [6-8] and electrophoretic [9, 10] separations. Their potential has
62 also been evaluated in the microextraction context [11-14].

63 Carbon nanoparticles (CNPs) have been extensively used in microextraction techniques
64 thanks to their outstanding sorbent capacity [15]. This property is usually ascribed to the
65 high surface to volume ratio of the nanomaterials. However, a relevant disadvantage of

66 using CNPs as sorbent, and carbon nanotubes in particular, is their aggregation tendency
67 due to their low solubility in common organic solvents and water. This fact hinders their
68 use in conventional cartridge-SPE formats and also limits their packing in microcolumn
69 inserted in flow configurations because of the high back-pressure generated. Therefore, in
70 order to benefit from their sorbent capacity, CNPs have to be efficiency dispersed or
71 immobilized on a surface/support, such as disk [16], controlled-pore glass [17] or porous-
72 hollow fiber [18] to minimize or avoid the presence of aggregates.

73 Although there are references dealing with the use of nanoparticles to improve the
74 chromatographic or electrophoretic separations [19-23], the combination of nanoparticles
75 and monolithic solids as extraction phase is scarcely reported [24-26]. In the particular case
76 of multi-walled carbon nanotubes (MWCNTs), they exhibit limited solubility in most of the
77 porogen solvents used for the synthesis of the monolith. Aggregates of MWCNTs are
78 observed even at very low concentrations in the polymerization mixture.

79 This study evaluates the potential of a poly(butyl acrylate-*co*-ethyleneglycol
80 dimethacrylate) monolithic capillary modified with carboxylated multi-walled carbon
81 nanotubes as a microextraction unit for preconcentration of triazine herbicides (prometon,
82 simazine, atrazine, propazine, terbumeton, secbumeton, simetryn, prometryn and terbutryn)
83 from waters and orange juices. The preparation of the hybrid solid has been deeply studied
84 as well as all the variables affecting the microextraction process. Gas chromatography with
85 mass spectrometric detection was used for analytes identification and quantification.

86 **Experimental section**

87 *Reagents, materials and samples*

88 All reagents were of analytical grade or better. Triazines (prometon, simazine, atrazine,
89 propazine, terbumeton, secbumeton, simetryn, prometryn and terbutryn) were purchased
90 from Sigma-Aldrich (Madrid, Spain. <http://www.sigmaaldrich.com>). Standard solutions of
91 each analyte were prepared in methanol (Sigma-Aldrich) at a concentration of $1 \text{ g}\cdot\text{L}^{-1}$ and
92 stored at $4 \text{ }^\circ\text{C}$. Working standard solutions were prepared on a daily basis by rigorous
93 dilution of the stocks in ultrapure Milli-Q water. Methanol was also used for triazines
94 elution.

95 Uncoated fused-silica capillaries ($320 \text{ }\mu\text{m}$ i.d., Sigma Aldrich) were used for the
96 preparation of the monolithic extraction unit. Ferrules 1/16" ID, PEEK tubing 1/16" and
97 internal union zero volume 1/16" to 1/16" (Sigma-Aldrich) were also employed.

98 The reagents used for the synthesis of the monolithic phase, butyl acrylate (BA),
99 ethyleneglycol dimethacrylate (EGDMA), lauroyl peroxide (LPO), 2-propanol (2-PrOH),
100 formamide, 3-(trimethoxysilyl)propyl methacrylate, ethanol, sodium hydroxide,
101 hydrochloric acid, acetone and acetic acid were purchased from Sigma-Aldrich.
102 Carboxylated multi-walled carbon nanotubes (c-MWCNTs, $< 8 \text{ nm}$ o.d., $10\text{-}30 \text{ }\mu\text{m}$ length,
103 $> 95 \text{ wt}\%$ purity, $3.86 \text{ wt}\%$ functional content) and carboxylated single-walled carbon
104 nanotubes (c-SWCNTs, $1\text{-}2 \text{ nm}$ o.d., $5\text{-}30 \text{ }\mu\text{m}$ length, $>90 \text{ wt}\%$ purity, $2.73 \text{ wt}\%$ functional
105 content) were obtained from Sigma-Aldrich. Single-walled nanohorns were purchased from
106 Carbonium S.r.l (Padua, Italy. <http://www.carbonium.it/public/site/index.php>). The
107 production of SWNHs was carried out, according to the information reported by the
108 manufacturer, by direct graphite evaporation in Ar flow and the purity obtained was above
109 $90 \text{ wt}\%$. SWNHs form stable dahlia-shaped aggregates with an average diameter of $60\text{-}80$
110 nm. Individually, the lengths of these SWNHs are in the range of 40 to 50 nm , and the

111 diameter in the cylindrical structure varies between 4-5 nm. Table S1 presents the
112 schematic structure as well as the TEM micrographs obtained for the three carbon
113 nanoparticles used in this article. A 7% (v/v) aqueous solution of ethylenediamine (Sigma-
114 Aldrich) was used to immobilize the c-MWCNTs on the monolith.

115 The dispersion of the c-MWCNTs was made in ethanol. In brief, 0.5 mg of c-MWCNTs
116 were weighed, added to a glass vial and ultrasonic-assisted dispersed in 50 mL of ethanol
117 for 30 min.

118 Tap and river water samples were selected for the determination of the target compounds
119 using the monolithic microextraction unit. Water samples from the Guadalquivir river were
120 collected in amber glass bottles (Sigma-Aldrich) without headspace and stored at 4 °C until
121 analysis. All the aliquots were filtered using a 0.45 µm disposable Nylon filter (Análisis
122 Vínicos, Córdoba, Spain. <http://www.analisisvinicos.com>) prior to analysis. The water
123 samples were prepared with the analytes at a concentration of 1 µg·L⁻¹, and then they were
124 left to stand for 24 h prior to the analysis. The oranges and juice samples were purchased
125 from local markets and stored at 4 °C until their use. The squeezed juice was prepared in
126 the laboratory prior to analysis. 1 mL of both orange juices were diluted with Milli-Q water
127 to 5 mL and filtered through a 0.20 µm disposable Nylon filter prior to the analysis.

128

129 *Apparatus*

130 SP-400 NanobaumeTM System (<http://www.chromatography.hplcsupply.com>) was used to
131 pump the c-MWCNTs dispersion through the monolithic microextraction unit. For analytes
132 preconcentration and elution, a micro-HPLC pump Jasco 1585 (Jasco Analítica Spain,

133 Madrid, Spain. <http://www.jasco-spain.com>) was employed. The poly(BA-co-EGDMA-co-
134 MWCNTs) microextraction unit was connected to the pump by means of a stainless steel
135 internal union fitted with a PEEK adapter.

136 Chromatographic analyses were carried out on a gas chromatograph (Varian CP-3800)-
137 mass spectrometer (Varian 1200 MS/MS) working under single quadrupole mode and with
138 an electron multiplier detector. The gas chromatograph was equipped with a fused silica
139 capillary column VF-5 ms (30 m x 0.25 mm i.d.) coated with 5 % phenyl-95 %
140 dimethylpolysiloxane (film thickness 0.25 μm) (Sigma-Aldrich) to separate the nine
141 analytes. The GC oven was programmed as follows: the initial temperature, 40 $^{\circ}\text{C}$, was
142 maintained for 2 min, raised up to 170 $^{\circ}\text{C}$ at 10 $^{\circ}\text{C}\cdot\text{min}^{-1}$ and then immediately ramped at 2
143 $^{\circ}\text{C}\cdot\text{min}^{-1}$ up to 200 $^{\circ}\text{C}$. The final temperature, 260 $^{\circ}\text{C}$, was reached with a ramp of 10
144 $^{\circ}\text{C}\cdot\text{min}^{-1}$ and maintained for 2 min. The injector temperature was 280 $^{\circ}\text{C}$ and the splitless
145 mode was selected. The injection volume, 2 μL of methanol, was measured with a 5 μL
146 microsyringe (Hamilton Co., Nevada, USA). The carrier gas used was helium (6.0 grade,
147 Air Liquide, Seville, Spain) at a flow rate of 1.0 $\text{mL}\cdot\text{min}^{-1}$, and it was regulated by digital
148 pressure controller. The transfer line and ionization source were maintained at 280 $^{\circ}\text{C}$ and
149 250 $^{\circ}\text{C}$, respectively.

150 The ionization mode employed in the mass spectrometer was electron impact (EI) with
151 ionization energy of 70 eV. Mass spectra were acquired using the selected ion monitoring
152 mode (SIM), dividing the analysis time in four temporal windows: the first one with m/z
153 200, 201, 210 and 214 (from 9 to 12.15 min), the second one selecting the m/z 196 (from
154 12.15 to 13.72 min), the third one with m/z 213 and 241 (from 12.15 to 15.45) and the
155 fourth temporal window selecting m/z 226 (15.45 to 28.25), all of them at 1 scan/s.

156 Chromatograms were acquired and processed using MS Workstation on an AMD
157 Sempro™ Processor computer (<https://www.bruker.com>) which also controlled the whole
158 system.

159 A JEOL JSM 6300 scanning electron microscopy (Isaza, Alcobendas, Spain) was also used
160 to obtain the micrographs of the monolithic solid with and without carbon nanoparticles.
161 An ultrasonic bath model 3510 from Branson (Connecticut, USA) was also used in
162 different steps of the procedure. In the preparation of the poly(BA-co-EGDMA) monolithic
163 capillary, an oven (Binder, Madrid, Spain) was also needed to maintain the temperature at
164 70 °C during the polymerization step.

165 *Preparation of monolithic solid*

166 The fused-silica capillary was pretreated to favor the covalent binding of the monolithic
167 phase to the capillary inner wall [19]. For this aim, the capillary (1 m in length) was flushed
168 with acetone (5 min) and Milli-Q water (20 min) at a flow rate of 1 mL·min⁻¹. NaOH (0.2
169 M) was sequentially pumped through the capillary using the micro-HPLC pump for 30 min
170 at a flow rate of 50 µL·min⁻¹. Then, the capillary was rinsed with Milli-Q water (1 mL·min⁻¹
171 ¹, 20 min), and then a 0.2 M HCl stream was passed for 30 min (50 µL·min⁻¹) to protonate
172 the silanol groups previously formed. Next, the acid was removed with Milli-Q water and
173 ethanol (1 mL·min⁻¹, 30 min), followed by a 20% (v/v) solution of 3-
174 (trimethoxysilyl)propyl methacrylate in ethanol (adjusted to pH 5 using acetic acid) at a
175 flow rate of 50 µL·min⁻¹ (45 min). Finally, the capillary was washed with acetone (1
176 mL·min⁻¹, 20 min) and dried under a nitrogen stream. The whole pretreatment of fused-

177 silica capillary was performed at room temperature. Pieces of 3 cm were then used to
178 synthesize the monolith.

179 The polymerization mixture is composed of 20 wt% monomers (25 wt% BA and 75 wt%
180 EGDMA) and 80 wt% porogens (50 wt% 2-PrOH and 50 wt% formamide). As free-radical
181 initiator, 0.3 wt% of LPO (out of the total weight of monomers) was added to the
182 polymerization mixture. This reaction mixture was sonicated for 20 min and purged with
183 nitrogen for 10 min. A piece of the pretreated fused-silica capillary (3 cm in length) was
184 filled with the reactant solution by means of a syringe and then sealed with a septum at both
185 ends. Next, the capillary was introduced into an oven at 70 °C for 24 h. After completing
186 the polymerization reaction, poly(BA-*co*-EGDMA) monolith was washed with methanol to
187 remove the unreacted monomers and porogenic solvents.

188 *Immobilization of carboxylated multi-walled carbon nanotubes on the monolith*

189 In order to immobilize the carbon nanoparticles on the monolithic solid, primary amine
190 functional groups were generated on its pores and surface [27]. For this purpose, an
191 ethanolic solution of ethylenediamine (7% (v/v)) was pumped through the capillary for 90
192 min at a flow rate of 50 $\mu\text{L}\cdot\text{min}^{-1}$. Then, the capillary was washed with water to neutral pH
193 for 30 min at a flow rate 0.3 $\text{mL}\cdot\text{min}^{-1}$.

194 Next, the poly(BA-*co*-EGDMA) monolith was dried under a nitrogen stream and an
195 ethanolic dispersion of 0.01 $\text{g}\cdot\text{L}^{-1}$ of the c-MWCNTs was pumped at a flow rate of 0.3
196 $\text{mL}\cdot\text{min}^{-1}$ for 5 min under continuous stirring using the set-up represented in Fig. 1A.
197 Micrographs of the cross-section of monolithic capillary columns (320 μm i.d.) were
198 obtained for the poly(BA-*co*-EGDMA) monolith (Fig. 2A) and the poly(BA-*co*-EGDMA-
199 c-MWCNTs) monolith (Fig. 2B). The micrographs were obtained using scanning electron

200 microscopy. The section of the capillaries was coated with gold to increase the
201 conductivity. The presence of the nanoparticles was corroborated by comparing both
202 micrographs.

203

204 *Microextraction procedure*

205 The poly(BA-*co*-EGDMA-*c*-MWCNTs) monolith was used for the isolation and
206 preconcentration of triazine herbicides from waters and juices. The microextraction is
207 schematically depicted in Fig.1B and it is as follows. First, 3 mL of aqueous standards or
208 samples containing the nine target analytes at concentrations within the linear range were
209 passed through the microextraction unit at a flow rate of 0.3 mL·min⁻¹ for 10 min, followed
210 by Milli-Q water (3 min). Prior to elution, the aqueous phase remaining in the column was
211 removed by means of a nitrogen stream (10 min). After that, the retained analytes were
212 eluted with 200 µL of methanol at flow rate of 0.1 mL·min⁻¹. An evaporation–redissolution
213 step was included in order to reduce the final volume to 20 µL, thus increasing the method
214 sensitivity. Finally, 2 µL of the organic phase with the extracted analytes were injected into
215 the gas chromatograph/mass spectrometer for their separation and detection. The
216 chromatographic peak areas were used as analytical signals. Between samples, the
217 poly(BA-*co*-EGDMA-*c*-MWCNTs) monolith was conditioned with methanol (1.3 mL, 0.1
218 mL·min⁻¹), dried with a nitrogen stream for 10 min and finally rinsed out with Milli-Q
219 water. Following this procedure, the monolithic capillary can be reused for 20 times
220 without efficiency losses. Longer uses reduce the extraction efficiencies in ca. 30%.

221

222 **Results and discussion**

223 *Variables affecting to the preparation of the poly(BA-co-EGDMA-c-MWCNTs) monolith*

224 The polymerization was carried out in one-step procedure using a 3 cm pretreated silica
225 capillary, mixing monomers, porogens and an initiator at 70 °C for 24 h. The temperature
226 and reaction time were fixed according to the indications of Viklund et al. [28]. The initial
227 experimental conditions were: 20 wt% monomers (50 wt% BA and 50 wt% EGDMA) and
228 80 wt% porogens (50 wt% 2-PrOH and 50 wt% formamide). A solution of LPO (0.3 wt%
229 out of the total weight of the monomers) was used as an initiator of the reaction. The
230 poly(BA-co-EGDMA) monolithic capillary was evaluated using the determination of
231 triazine herbicides as model compounds. For this purpose, 4.8 mL of a working standard
232 solution containing the nine analytes at a concentration of 1 $\mu\text{g}\cdot\text{mL}^{-1}$ was preconcentrated,
233 using methanol as eluent. Three replicate analyses for each monolithic column to evaluate
234 also the repeatability of the different extraction units.

235 The first variable studied was the monomers/porogens ratio within the following
236 proportions: 20/80% (w/w), 40/60% (w/w), 60/40% (w/w) and 80/20% (w/w). The high
237 percentage of monomers resulted in the smaller pores and therefore it led to an increased
238 flow resistance. Thus a 20/80% (w/w) ratio was selected for further experiments.

239 Next, the BA/EGDMA ratio was studied within the following percentages: 75/25% (w/w),
240 60/40% (w/w), 40/60% (w/w) and 25/75% (w/w). When the ratio was 75/25% (w/w) the
241 resulting pores were too small and the high backpressure generated hindered the flow of
242 solvents through the capillary. However, although monoliths prepared with the other ratios
243 exhibited a favourable permeability to flow the solvents, the extraction efficiency of the
244 bare monolithic solid towards the triazines was very low as it shown in the Fig. 3A.

245 Therefore, the inclusion of carbon nanoparticles in the microextraction unit was deeply
246 studied, including both the type and their amount. For this purpose, commercially available
247 carboxylated carbon nanotubes (c-SWCNTs, c-MWCNTs) and laboratory-oxidized carbon
248 nanohorns (o-SWNHs) were selected taking into consideration their better dispersibility in
249 organic media [29].

250 Dispersions of each carbon nanoparticle were prepared at a concentration of $1 \text{ mg}\cdot\text{L}^{-1}$. A
251 volume of $900 \mu\text{L}$ was flushed through the monolithic capillary column at a flow rate of 0.3
252 $\text{mL}\cdot\text{min}^{-1}$ in order to retain the nanoparticles on the microporous material.

253 When the proportion was 60/40% (w/w), the monolithic solid was collapsed under pressure
254 during the procedure of the immobilization of the carbon nanoparticles. While for the ratios
255 40/60% (w/w) and 25/75% (w/w) it was possible to anchor the NPs on the monolithic
256 surfaces, obtaining a greater increase when the percentage of BA decreased as regards that
257 of the cross-linker. We attribute this to the highest adsorption on the largest pores when
258 dispersions of the NPs were passed through the monolithic solid. For this reason, the
259 selected ratio was 25/75% (w/w) of BA/EGDMA. Fig. 3A exemplified this behavior for c-
260 MWCNTs and terbutryn as model NPs and compound, respectively.

261 Besides, as it is shown in Fig. 3B, the presence of the c-MWCNTs, c-SWCNTs, and o-
262 SWNHs increased the retention of the triazines on the microextraction unit in comparison
263 with the bare monolithic solid. The best results were obtained using c-MWCNTs as
264 modifiers of the bare poly(BA-co-EGDMA) monolith. They exhibit the highest sorbent
265 capacity owing to their larger size and number of sheets in comparison with the other
266 carbon nanoparticles (c-SWCNTs and o-SWNHs). Also, the precision of the results ($n=3$)

267 expressed as standard deviation and reflected in the Fig. 3B as error bars, was better for
268 almost all the analytes. The better performance of o-SWNHs as regards c-SWCNTs can be
269 explained taking into consideration their ability to form stable large aggregates (60-80 nm)
270 which results in higher extraction capacity. From these results, c-MWCNTs were selected.

271 The influence of the amount of c-MWCNTs immobilized on the monolithic solid surface
272 was tested using ethanolic dispersions of the nanoparticles at concentrations of 0.001, 0.01
273 and 0.05 g·L⁻¹. Aliquots of 900 µL were passed through the column at a flow rate of 0.3
274 mL·min⁻¹. The highest concentration generated a backpressure in the system, probably due
275 to the aggregation of the nanoparticles which resulted in pores blockage. The results
276 obtained for the other two concentrations are shown in Fig. 4. As expected, the higher
277 amount of nanoparticles resulted in higher efficiency and therefore, a concentration of 0.01
278 g·L⁻¹ of the c-MWCNTs in ethanol was selected. This dispersion was flushed in an interval
279 from 3 to 25 min at a flow rate of 0.3 mL·min⁻¹ (0.9-7.5 mL). The graphic comparison of
280 the results given in Fig. 5, shows that 1.5 mL (5 min) was the best option since higher
281 values resulted in a decrease of the extraction, probably due to bundle formation on the
282 pore and surface of the monolith.

283 *Evaluation of the variables affecting to the microextraction process*

284 The variables directly related with the extraction step were studied using aqueous standards
285 containing the selected triazines at a concentration of 1 µg·mL⁻¹.

286 The following parameters were optimized: (a) Sample flow rate; (b) sample volume and;
287 (c) elution volume. Respective data and Figures are given in the *Electronic Supporting*
288 *Material*. The following experimental conditions were found to give the best results: (a) a

289 sample flow rate of $0.3 \text{ mL}\cdot\text{min}^{-1}$, (b) a sample volume of 3 mL and, (c) an elution volume
290 of 0.2 mL.

291

292 *Analytical figures of merit*

293 Once optimized, the monolithic extraction unit was characterized in terms of sensitivity,
294 linearity, and precision. The corresponding calibration graphs were constructed by using
295 aqueous standards containing the nine analytes at concentrations in the range $0.1\text{-}1000$
296 $\mu\text{g}\cdot\text{L}^{-1}$. Standards were processed in duplicate using the optimized method, and $2 \mu\text{L}$ of the
297 organic extract was injected into the GC/MS for analysis. The corresponding equations
298 were obtained by plotting the peak areas of the characteristic m/z fragment ions against the
299 concentration for each target analyte.

300 The limits of detection (LODs) were calculated as the concentrations giving a signal-to-
301 noise ratio (S/N) of 3. As it can be seen in Table 1, they were in the range $0.03\text{-}0.6 \mu\text{g}\cdot\text{L}^{-1}$.

302 The limits of quantification (LOQs) were calculated as the concentration providing
303 chromatographic peak areas ten times higher than the background noise and varied between
304 0.1 and $0.4 \mu\text{g}\cdot\text{L}^{-1}$ for all analytes (simazine excepted, $1 \mu\text{g}\cdot\text{L}^{-1}$). The precision of the
305 method (intra and inter-day conditions), expressed as relative standard deviation (RSD) was
306 calculated from five individual standards prepared at a concentration of $1 \mu\text{g}\cdot\text{mL}^{-1}$ and it
307 was lower than 11.4 % for all the analytes. Fig. 6 shows a chromatograph with the different
308 m/z fragment ions obtained after the analysis of a standard with the nine triazines ($1 \mu\text{g}\cdot\text{L}^{-1}$)
309 following the microextraction procedure. In addition, the reproducibility between extraction
310 units was evaluated. For this purpose, five poly(BA-*co*-EGDMA-*c*-MWCNTs) monolithic
311 microextraction units were prepared and a standard solution of the nine triazines ($1 \mu\text{g}\cdot\text{mL}^{-1}$)

312 ¹) was analyzed. The results, expressed as RSD, are also given in Table 1 and they were
313 acceptable in all cases.

314 *Analysis of water and orange juice samples*

315 Prior to the analysis of real samples, the identification of potential interferences from the
316 matrix on the quantification of the analytes is a relevant issue, especially when analyzing
317 unknown samples. Therefore, the accuracy of the proposed method was evaluated through a
318 recovery study. As neither certified reference materials (CRMs) nor quality control (QC)
319 samples were available for this specific analytical problem, different blank water and juice
320 samples were fortified with the nine target analytes (prometon, simazine, atrazine,
321 propazine, terbumeton, secbumeton, simetryn, prometryn and terbutryn) at a concentration
322 of 1 $\mu\text{g}\cdot\text{L}^{-1}$, and they were left to stand for 24 h prior to analysis. Then, the fortified
323 samples were analyzed using the extraction method, and the concentration for each triazine
324 was calculated by interpolating the peak area obtained in the corresponding calibration
325 graph. The recovery values were calculated dividing the concentration found by the
326 concentration added, and expressed in percentage. Each sample was analyzed by triplicate;
327 the results obtained are listed in Table 2. As it can be seen, they were acceptable in all
328 instances and they are ranged from 75 to 125 %.

329 The extraction method was applied to the determination of the target triazines in two water
330 samples (river and tap waters) and two types of orange juice samples (squeezed and
331 commercial). Aliquots of 3 mL of water and juice samples were passed through the
332 poly(BA-co-EGDMA-c-MWCNTs) monolith and processed under the optimum conditions.
333 As a result, none of the analytes were found in waters and squeezed orange juices.

334 However, as it can be seen in Table 2 a low content of prometryn was detected in
335 commercial orange juices. Herbicide residues may be present in the juice made from
336 concentrate due to the great consumption on agrochemical for the protection of crops in
337 agriculture and they can be transferred from orange peels to juices.

338 **Conclusions**

339 The use of monolithic solids in the microextraction context has been recently reviewed
340 [14]. Table 3 summarizes the comparison of the present method with other monolithic
341 packings for the extraction and isolation of triazine herbicides from different samples. Most
342 of these extraction units are based on methacrylate monolithic columns, and LODs ranged
343 from 0.18 to 95.0 $\mu\text{g}\cdot\text{L}^{-1}$. The extraction of efficiency of these porous materials has been
344 enhanced by the incorporation of nanoparticles, and especially carbonaceous ones, in the
345 monolith. In this regard, carboxylated single-walled carbon nanotubes, have been used to
346 improve the sorption capacity of poly(MAA-*co*-EDMA) monoliths. In this approach, the
347 nanoparticles are added to the polymerization mixture in such a way that they are finally
348 embedded into the solid. This procedure presents as an advantage the higher stability of the
349 hybrid sorbent as the nanoparticles are included in the polymer. However, only those
350 nanoparticles remaining on the pores are available for interaction. In addition, nanoparticles
351 must be soluble in the polymerization mixture (usually the porogenic solvent) to minimize
352 the aggregation of the material. Moreover, avoiding the sedimentation of the nanomaterial
353 during polymerization also has to be taken into account in order to obtain a homogeneous
354 distribution.

355 The hybrid monolithic sorbent presented in this article [poly(BA-*co*-EGDMA-*c*-
356 MWCNTs)] overcomes these two shortcomings as the carbon nanoparticles are
357 immobilized on the monolithic sorbent previously formed. Therefore, LODs reached with
358 the present method were comparable with the poly(MAA-*co*-EDMA-SWNT) monolithic
359 approach. Also aggregation is reduced as they are prepared in an organic medium (ethanol)
360 where they are soluble. Besides we have evaluated the performance of three carbon
361 nanoparticles (*c*-SWCNTs, *o*-SWNHs and *c*-MWCNTs) as component of the monolithic
362 sorbent, showing the multi-walled structures the most favourable features in terms of
363 extraction efficiency.

364 This study, demonstrates that the immobilization of *c*-MWNTs onto the pore surface of
365 poly(BA-*co*-EGDMA) monoliths, significantly increases the extraction efficiency for the
366 target triazines. In addition, the microextraction method shows favorable analytical features
367 for the analytical problem selected.

368 **Acknowledgments**

369 Financial support from the Spanish Ministry of Science and Innovation (grant CTQ2011-
370 23790 and CTQ2014-52939-R) is gratefully acknowledged. B. Fresco-Cala expresses her
371 gratitude for the predoctoral grant (ref FPU13/03896) from the Spanish Ministry of
372 Education.

373

374

375

376 **References**

- 377 [1] Aziz-Zanjani MO, Mehdinia A (2014) A review on procedures for the preparation of
378 coatings for solid phase microextraction, *Microchim Acta* 181: 1169.
- 379 [2] Lucena R, Simonet B, Cárdenas S, Valcárcel M (2011) Potential of nanoparticles in
380 sample preparation, *J Chromatogr A* 1218: 620.
- 381 [3] Svec F (2010) Porous polymer monoliths: amazingly wide variety of techniques
382 enabling their preparation, *J Chromatogr A* 1217: 902.
- 383 [4] Núñez O, Nakanishi K, Tanaka N (2008) Preparation of monolithic silica columns for
384 high-performance liquid chromatography, *J Chromatogr A* 1191: 231.
- 385 [5] Ou J, Lin H, Zhang Z, Huang G, Dong J, Zou H (2013) Recent advances in preparation
386 and application of hybrid organic-silica monolithic capillary columns, *Electrophoresis* 34:
387 126.
- 388 [6] Liang Y, Zhang L, Zhang Y (2013) Recent advances in monolithic columns for protein
389 and peptide separation by capillary liquid chromatography, *Anal Bioanal Chem* 405: 2095.
- 390 [7] Nischang I, Teasdale I, Brüggemann O (2010) Towards porous polymer monoliths for
391 the efficient, retention-independent performance in the isocratic separation of small
392 molecules by means of nano-liquid chromatography, *J Chromatogr A* 1217: 7514.
- 393 [8] Kurganov A (2013) Monolithic column in gas chromatography, *Anal Chim Acta* 775:
394 25.
- 395 [9] Cantó-Mirapeix A, Herrero-Martínez JM, Mongay-Fernández C, Simó-Alfonso EF
396 (2009) CEC column behaviour of butyl and lauryl methacrylate monoliths prepared in
397 non-aqueous media, *Electrophoresis* 30: 607.

398 [10] Bernabé-Zafón V, Cantó-Mirapeix A, Simó-Alfonso EF, Ramis-Ramos G,
399 Herrero-Martínez JM (2009) Comparison of thermal-and photo-polymerization of lauryl
400 methacrylate monolithic columns for CEC, Electrophoresis 30: 1929.

401 [11] Galán-Cano F, Bernabé-Zafón V, Lucena R, Cárdenas S, Herrero-Martínez JM,
402 Ramis-Ramos G, Valcárcel M (2011) Sensitive determination of polycyclic aromatic
403 hydrocarbons in water samples using monolithic capillary solid-phase extraction and on-
404 line thermal desorption prior to gas chromatography–mass spectrometry, J Chromatogr A
405 1218: 1802.

406 [12] Mei M, Huang X, Yuan D (2014) Multiple monolithic fiber solid-phase
407 microextraction: A new extraction approach for aqueous samples, J Chromatogr A 1345:
408 29.

409 [13] Rahmi D, Takasaki Y, Zhu Y, Kobayashi H, Konagaya S, Haraguchi H, Umemura T
410 (2010) Preparation of monolithic chelating adsorbent inside a syringe filter tip for solid
411 phase microextraction of trace elements in natural water prior to their determination by
412 ICP-MS, Talanta 81: 1438.

413 [14] Huang X, Yuan D (2012) Recent developments of extraction and micro-extraction
414 technologies with porous monoliths, Crit Rev Anal Chem 42: 38.

415 [15] Fresco-Cala B, Jimenez-Soto JM, Cardenas S, Valcarcel M (2014) Single-walled
416 carbon nanohorns immobilized on a microporous hollow polypropylene fiber as a sorbent
417 for the extraction of volatile organic compounds from water samples, Microchim Acta 181:
418 1117.

419 [16] Roldán-Pijuán M, Lucena R, Cárdenas S, Valcárcel M (2014) Micro-solid phase
420 extraction based on oxidized single-walled carbon nanohorns immobilized on a stir

421 borosilicate disk: Application to the preconcentration of the endocrine disruptor
422 benzophenone-3, *Microchem J* 115: 87.

423 [17] Suárez B, Simonet B, Cárdenas S, Valcárcel M (2007) Determination of non-steroidal
424 anti-inflammatory drugs in urine by combining an immobilized carboxylated carbon
425 nanotubes minicolumn for solid-phase extraction with capillary electrophoresis-mass
426 spectrometry, *J Chromatogr A* 1159: 203.

427 [18] Es'haghi Z, Ebrahimi M, Hosseini M-S (2011) Optimization of a novel method for
428 determination of benzene, toluene, ethylbenzene, and xylenes in hair and waste water
429 samples by carbon nanotubes reinforced sol-gel based hollow fiber solid phase
430 microextraction and gas chromatography using factorial experimental design, *J Chromatogr*
431 *A* 1218: 3400.

432 [19] Chambers SD, Svec F, Fréchet JM (2011) Incorporation of carbon nanotubes in porous
433 polymer monolithic capillary columns to enhance the chromatographic separation of small
434 molecules, *J Chromatogr A* 1218: 2546.

435 [20] Li Y, Chen Y, Xiang R, Ciuparu D, Pfefferle LD, Horváth C, Wilkins JA (2005)
436 Incorporation of single-wall carbon nanotubes into an organic polymer monolithic
437 stationary phase for μ -HPLC and capillary electrochromatography, *Anal Chem* 77: 1398.

438 [21] Thabano JR, Breadmore MC, Hutchinson JP, Johns C, Haddad PR (2009) Silica
439 nanoparticle-templated methacrylic acid monoliths for in-line solid-phase extraction-
440 capillary electrophoresis of basic analytes, *J Chromatogr A* 1216: 4933.

441 [22] Hilder EF, Svec F, Fréchet JM (2004) Latex-functionalized monolithic columns for the
442 separation of carbohydrates by micro anion-exchange chromatography, *J Chromatogr A*
443 1053: 101.

444 [23] Zakaria P, Hutchinson JP, Avdalovic N, Liu Y, Haddad PR (2005) Latex-coated
445 polymeric monolithic ion-exchange stationary phases. 2. Micro-ion chromatography, Anal
446 Chem 77: 417.

447 [24] Tong S, Liu Q, Li Y, Zhou W, Jia Q, Duan T (2012) Preparation of porous polymer
448 monolithic column incorporated with graphene nanosheets for solid phase microextraction
449 and enrichment of glucocorticoids, J Chromatogr A 1253: 22.

450 [25] Krenkova J, Foret F (2011) Iron oxide nanoparticle coating of organic polymer-based
451 monolithic columns for phosphopeptide enrichment, J Sep Sci 34: 2106.

452 [26] Wang X, Li X, Li Z, Zhang Y, Bai Y, Liu H (2014) Online coupling of in-tube solid-
453 phase microextraction with direct analysis in real time mass spectrometry for rapid
454 determination of triazine herbicides in water using carbon-nanotubes-incorporated polymer
455 monolith, Anal Chem 86: 4739.

456 [27] Tong S, Zhou X, Zhou C, Li Y, Li W, Zhou W, Jia Q (2013) A strategy to decorate
457 porous polymer monoliths with graphene oxide and graphene nanosheets, Analyst 138:
458 1549.

459 [28] Viklund C, Svec F, Fréchet JM, Irgum K (1996) Monolithic, “molded”, porous
460 materials with high flow characteristics for separations, catalysis, or solid-phase chemistry:
461 control of porous properties during polymerization, Chem Mater 8: 744.

462 [29] Jiménez-Soto JM, Cárdenas S, Valcárcel M (2013) Oxidized single-walled carbon
463 nanohorns as sorbent for porous hollow fiber direct immersion solid-phase microextraction
464 for the determination of triazines in waters, Anal Bioanal Chem 405: 2661.

465 [30] Su R, Liu Q, Fan S, Ma H, Zhou X, Jia Q (2012) Application of polymer monolith
466 microextraction to the determination of triazines in cereal samples combined with high-
467 performance liquid chromatography, Food Anal Methods 5: 1040.

468 [31] Chen J, Bai L, Tian M, Zhou X, Zhang Y (2014) Hollow-fiber membrane tube
469 embedded with a molecularly imprinted monolithic bar for the microextraction of triazine
470 pesticides, *Anal Methods* 6: 602.

471 [32] Djozan D, Ebrahimi B (2008) Preparation of new solid phase micro extraction fiber on
472 the basis of atrazine-molecular imprinted polymer: Application for GC and GC/MS
473 screening of triazine herbicides in water, rice and onion, *Anal Chim Acta* 616: 152.

474 [33] Djozan D, Farajzadeh MA, Sorouraddin SM, Baheri T, Norouzi J (2012) Inside-needle
475 extraction method based on molecularly imprinted polymer for solid-phase dynamic
476 extraction and preconcentration of triazine herbicides followed by GC–FID determination,
477 *Chromatographia* 75: 139.

478 [34] Djozan D, Mahkam M, Ebrahimi B (2009) Preparation and binding study of solid-
479 phase microextraction fiber on the basis of ametryn-imprinted polymer: application to the
480 selective extraction of persistent triazine herbicides in tap water, rice, maize and onion, *J*
481 *Chromatogr A* 1216: 2211.

482

483

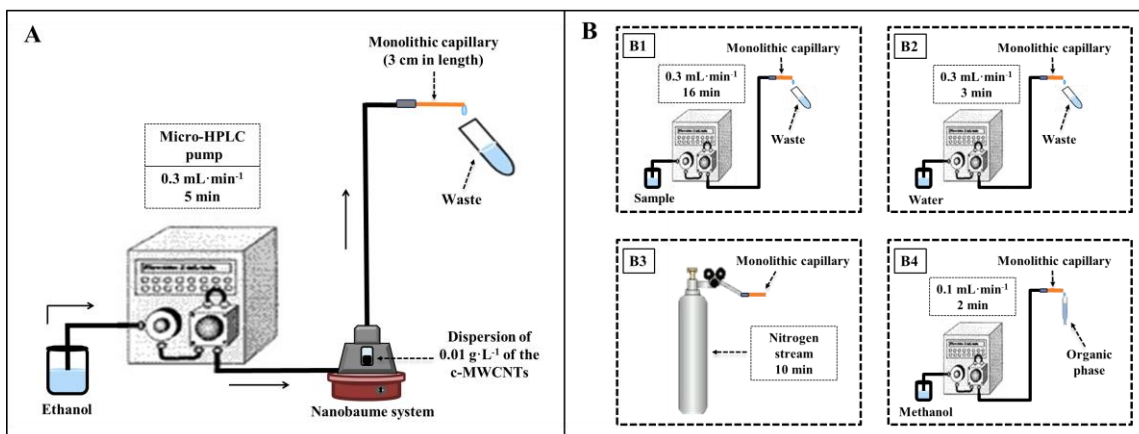
484

485

486

487

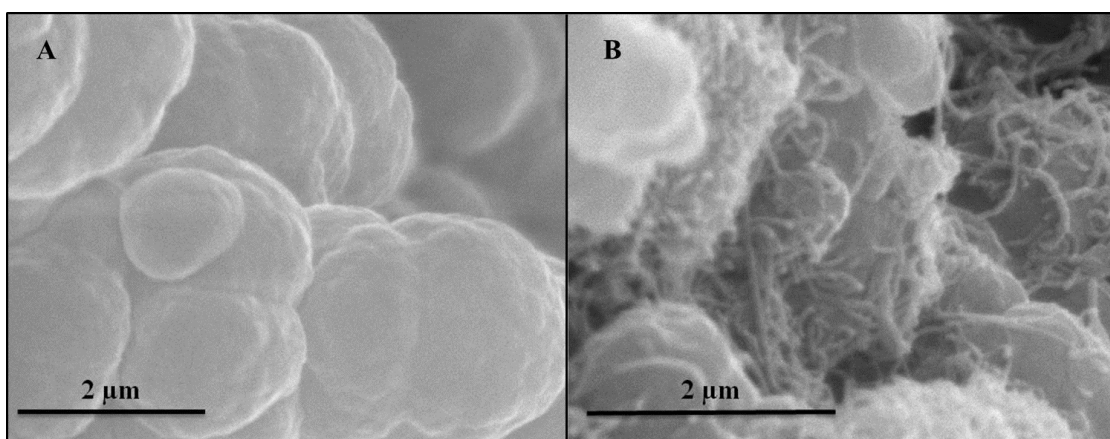
488



490

491 Fig. 1 (A) Instrumental set-up used for the immobilization of c-MWCNTs on the
 492 monolithic capillary. (B) Schematic representation of the microextraction procedure for the
 493 extraction of the triazine herbicides from waters and orange juice; (B1) sampling, (B2)
 494 washing, (B3) drying, and (B4) desorption.

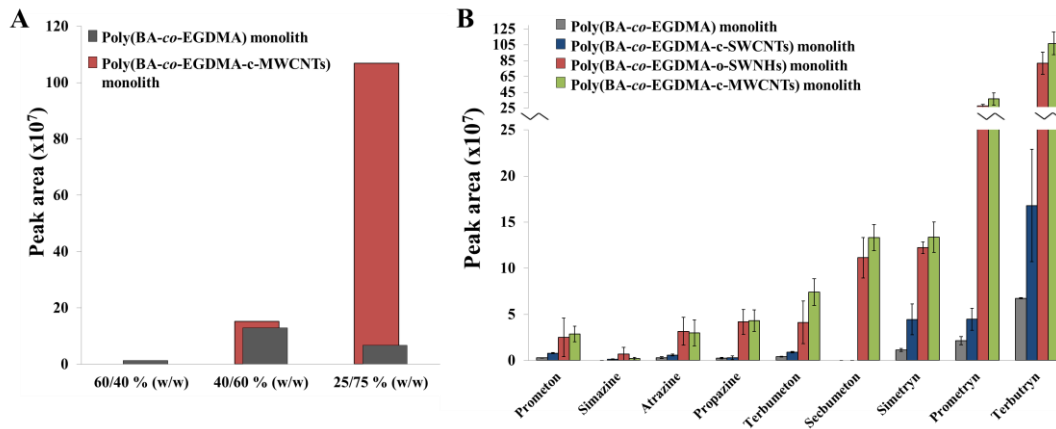
495



496

497 Fig. 2 (A, x15000) Scanning electron microscopy of poly(BA-co-EGDMA) and (B,
 498 x20000) poly(BA-co-EGDMA-c-MWCNTs) monolith.

499

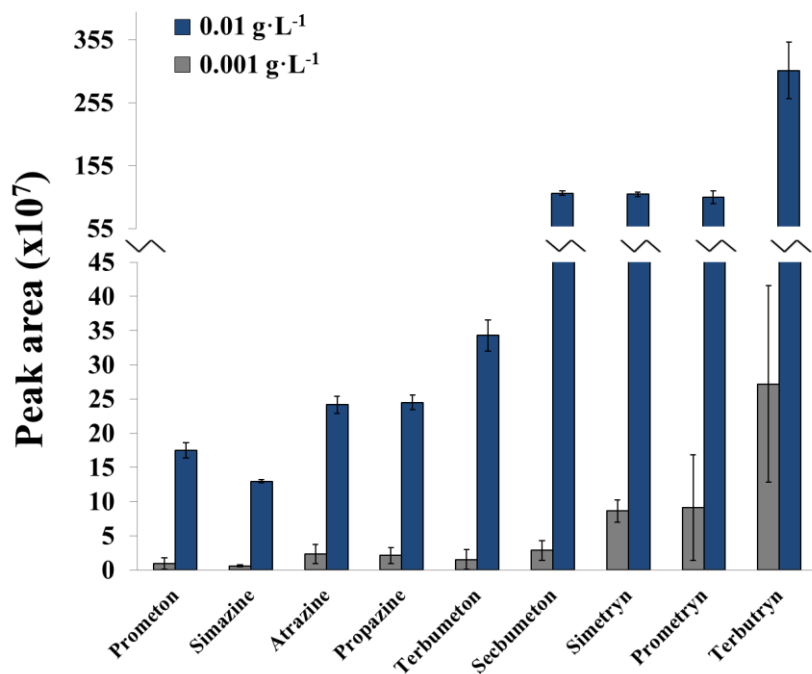


500

501 Fig. 3 (A) The relative extraction efficiency for terbutryn as model compound, using the
 502 bare poly(BA-co-EGDMA) monolith and the poly(BA-co-EGDMA-c-MWCNTs) monolith
 503 as microextraction unit. (B) Comparison of the analytical performance of poly(BA-co-
 504 EGDMA) monolith without nanoparticles and the monolith with c-MWCNTs, o-SWNHs
 505 and c-MWCNTs immobilized on its pores for 20/80 % (w/w) and 25/75% (w/w)
 506 proportions of monomers/porogens and monomers/cross-linker ratios, respectively.

507

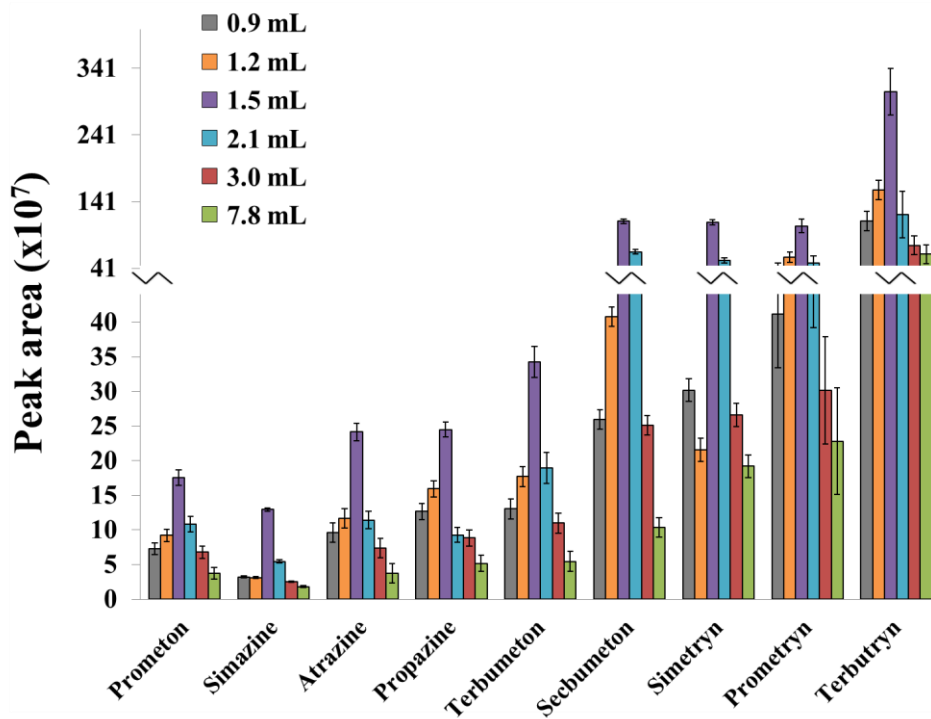
508



509

510 Fig. 4 Influence of the concentration of the c-MWCNTs dispersion on the triazines
 511 retention.

512

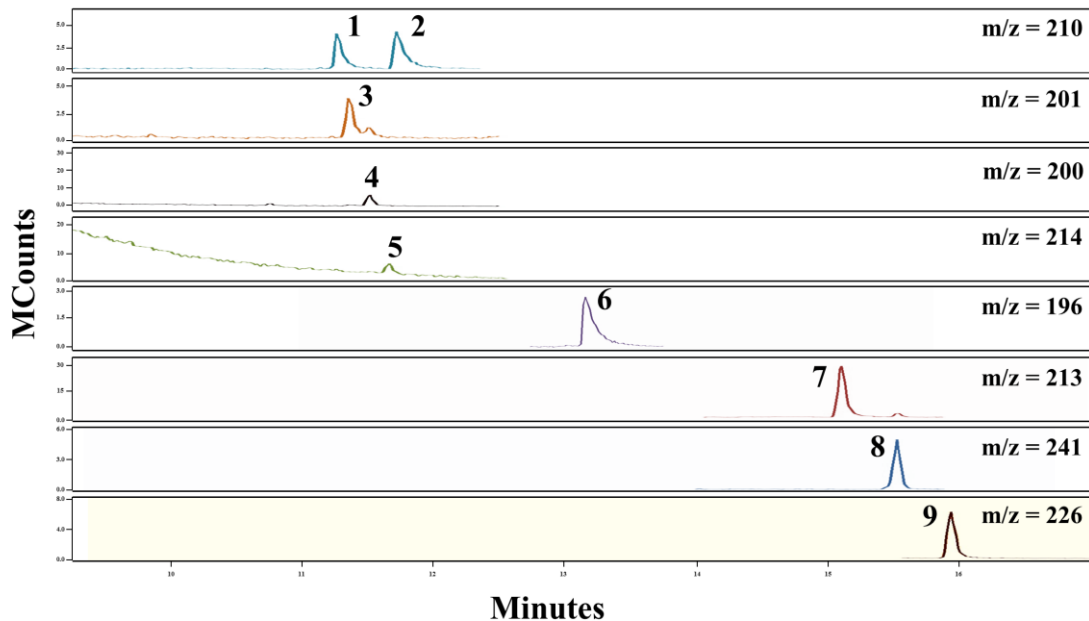


513

514 Fig. 5 Effect of the volume of the 0.01 g·L⁻¹ c-MWCNTs dispersion passed through the
 515 poly(BA-co-EGDMA) monolith at a flow rate of 0.3 mL·min⁻¹.

516

517



518

519 Fig. 6 Chromatogram obtained after monolith microextraction of a standard with the target
 520 analytes at a concentration of $1 \mu\text{g}\cdot\text{L}^{-1}$. Peaks: (1) Prometon, (2) Terbumeton, (3) Simazine,
 521 (4) Atrazine, (5) Propazine, (6) Secbumeton, (7) Simetryn, (8) Prometryn, (9) Terbutryn.

522

523

524

525

526

527

528

529 Table 1. Analytical figures of merit of poly(BA-co-EGDMA-c-MWCNTs) monolithic
 530 microextraction unit to the determination of the target triazines.

Analyte	m/z	LOD ($\mu\text{g}\cdot\text{L}^{-1}$)	LOQ ($\mu\text{g}\cdot\text{L}^{-1}$)	Precision		
				Intra- day RSD (%, n=5)	Inter- day RSD (%, n=5)	Inter- units RSD (%, n=5)
Prometon	210	0.10	0.4	9.4	11.4	6.8
Simazine	201	0.60	1	4.2	7.1	7.9
Atrazine	200	0.10	0.4	11.4	9.9	3.9
Propazine	214	0.10	0.4	6.0	5.3	8.2
Terbumeton	210	0.10	0.4	7.2	10.3	8.7
Sebumeton	196	0.03	0.1	3.0	7.4	10.0
Simetryn	213	0.03	0.1	4.1	8.6	9.0
Prometryn	241	0.03	0.1	5.9	8.1	13.8
Terbutryn	226	0.03	0.1	10.5	11.3	14.3

531 *LOD limit of detection, LOQ limit of quantification, RSD relative standard deviation*

532

533

534 Table 2. Recovery study for prometon, simazine, atrazine, propazine, terbumeton, secbumeton, simetryn, prometryn and terbutryn
 535 spiked to water samples and orange juices analyzed following c-MWCNTs monolithic extraction unit.

Analytes	Spiked ($\mu\text{g}\cdot\text{L}^{-1}$)	Tap water		River water		Commercial orange juice		Squeezed orange juice	
		Detected ($\mu\text{g}\cdot\text{L}^{-1}$)	Recoveries (%, n=3)	Detected ($\mu\text{g}\cdot\text{L}^{-1}$)	Recoveries (%, n=3)	Detected ($\mu\text{g}\cdot\text{L}^{-1}$)	Recoveries (%, n=3)	Detected ($\mu\text{g}\cdot\text{L}^{-1}$)	Recoveries (%, n=3)
Prometon	0	ND		ND		ND		ND	
	1	1.07	107 ± 11	0.85	85 ± 8	1.06	106 ± 10	0.84	84 ± 11
Simazine	0	ND		ND		ND		ND	
	1	1.11	111 ± 9	0.95	95 ± 7	0.75	75 ± 9	1.25	125 ± 10
Atrazine	0	ND		ND		ND		ND	
	1	0.80	80 ± 7	0.81	81 ± 11	1.03	103 ± 10	1.25	125 ± 11
Propazine	0	ND		ND		ND		ND	
	1	0.87	97 ± 8	0.96	96 ± 3	0.75	75 ± 10	0.94	94 ± 11
Terbumeton	0	ND		ND		ND		ND	
	1	1.13	113 ± 15	0.85	85 ± 9	0.91	91 ± 10	0.76	76 ± 10
Secbumeton	0	ND		ND		ND		ND	
	1	0.89	89 ± 10	0.87	87 ± 16	1.49	121 ± 8	0.76	76 ± 8
Simetryn	0	ND		ND		ND		ND	
	1	0.99	99 ± 5	0.98	98 ± 8	0.98	98 ± 6	1.21	121 ± 8
Prometryn	0	ND		ND		0.18		ND	
	1	0.81	81 ± 14	0.98	98 ± 14	1.18	100 ± 13	0.98	98 ± 12
Terbutryn	0	ND		ND		ND		ND	
	1	0.93	93 ± 5	1.01	101 ± 8	0.99	99 ± 13	1.15	115 ± 14

536

537 *ND: not detected*

538

539

540

541

542

543

544

545

546

547

548

549

550 Table 3. Comparison of the performance of the poly(BA-*co*-EGDMA-*c*-MWCNTs) monolith versus other monolithic sorbent
551 described in the literature for the determination of triazine herbicides.

Monolithic sorbent	Selected triazines	Packing	Sample	Limit of detection (LODs)	Precision (RSD, %)	Recovery (%)	Reference
Poly(MAA- <i>co</i> -EDMA-SWCNT) monolith	Simazine, atrazine, prometon, ametryn, propazine, and prometryne	Monolithic capillary column	Lake water and orange juice	0.02-0.14 $\mu\text{g}\cdot\text{L}^{-1}$	3.1-10.9	85.0-106.0	[26]

Poly(MAA-co-EGDMA) monolith	Cyanazine, simazine, atrazine, prometon, ametryn, and prometryn	Monolithic capillary column	Cereals	1.1-2.8 $\mu\text{g}\cdot\text{kg}^{-1}$	1.4-5.5	73.4-107.2	[30]
Poly(MAA-co-EDMA) monolith	Atrazine, 2-amino-4-methoxy-6-methyl-1,3,5-triazine, terbutylazine, and ametryn	Monolithic MIP-SPME fiber	Lake water	0.18-0.35 $\mu\text{g}\cdot\text{L}^{-1}$	5.3-12.0	72.8-113.2	[31]
Poly(MAA-co-EGDMA) monolith	Atrazine, simazine, propazine, cyanazine, ametryn, terbutryn, and prometryn	Monolithic MIP-SPME fiber	Tap water, onion and rice	20.0-88.0 $\mu\text{g}\cdot\text{L}^{-1}$	6.5-11.6	87.8-99.6	[32]
Poly(MAA-co-EGDMA) monolith	Atrazine, simazine, cyanazine, ametryn, prometryn and terbutryn	Monolithic MIP-SPME fiber	Grape juice, tap water and groundwater.	2.6-42.0 $\mu\text{g}\cdot\text{L}^{-1}$	4.4-12.1	82.1-93.5	[33]
Poly(MAA-co-EDMA) monolith	Ametryn, prometryn, terbutryn, atrazine, simazine, propazine, and cyanazine	Monolithic MIP-SPME fiber	Tap water, rice, maize and onion	14.0-95.0 $\mu\text{g}\cdot\text{L}^{-1}$	5.2-11.8	85.1-99.8	[34]
Poly(BA-co-EGDMA-c-MWCNTs) monolith	Prometon, terbumeton, simazine, atrazine, propazine, secbumeton, simetryn, prometryn, terbutryn	Monolithic capillary column	Tap and river water, and orange juice	0.03-0.1 $\mu\text{g}\cdot\text{L}^{-1}$	3.0-11.4	75.0-125.0	Present work